JST: Engineering and Technology for Sustainable Development
Volume 34, Issue 5, November 2024, 001-010

Optimal Extraction and Spray-Drying Anthocyanin from *Perilla Frutescens*

Hoang Thi Ngoc Nhon, Nguyen Thi Que Tran, Nguyen Minh Phuc, Tran Thi Huyen Linh, Le Thi Hong Anh*

Food Science and Technology, Ho Chi Minh City University of Industry and Trade, Ho Chi Minh City, Vietnam
**Corresponding author email: anhlth@huit.edu.vn*

Abstract

Perilla frutescens has been commonly used as a food ingredient and in folk medicine. Anthocyanins, with many biological activities, have potential applications in food and pharmaceuticals. This study aimed to determine the optimal conditions for anthocyanin extraction with solvents before investigating the effects of spray drying conditions to obtain anthocyanin powder. The result shows that 72% ethanol at 63 °C in 90 min resulted in the optimal anthocyanin content of 3.373 mg/g DM. The suitable conditions for spray-drying to obtain anthocyanin powder were at 160 °C with an input flow rate of 7 mL/min and a carrier agent concentration of 25%. A scanning electron microscope (SEM), X-ray radiation (XRD), and Fourier-transform infrared spectroscopy (FT-IR) confirmed effective microencapsulation, providing a basis for further research and applications of anthocyanin powder from this material.

Keywords: Anthocyanin, *Perilla frutescens*, solvent, spray-drying.

1. Introduction

In recent years, perilla leaves have gained increasing attention for their use as a health-boosting beverage. *Perilla frutescens* is mainly grown in countries such as China, Japan, India, Thailand, and South Korea, and is a very popular leaf resilient and well-suited to the hot climate of Vietnam. Recently, *P. frutescen* has been gaining more attention due to its healing benefits and plant chemical content. Perilla leaves are esteemed not only for their culinary applications but also for their potential health-promoting properties. This is attributed to their rich composition of essential oils, polyphenols, anthocyanins, omega-3 fatty acids, vitamins, and minerals [1]. The flowers contain a substantial number of anthocyanins, potent antioxidants that have positive effects on a range of conditions such as cardiovascular diseases, aging prevention, and cancer risk reduction. Additionally, anthocyanins inhibit lipid peroxidation reactions, preventing the accumulation of fats in internal organs, thus helping to maintain a slim figure and avoid obesity [2].

Anthocyanins are water-soluble pigments found in most vascular plants and have been utilized in many fields due to their positive impact on human health. No adverse effects from anthocyanin derivatives have been reported, even after the ingestion of very high doses [3]. Daily diets rich in anthocyanins have garnered significant attention within the community due to their beneficial effects, including anti-inflammatory, anti-diabetic, anti-cardiovascular, and antioxidant activities. Consequently, there is a growing demand for more sources of anthocyanins and improved extraction processes to meet the increasing requirements. Additionally, commercial applications of anthocyanins as colorants and pharmaceuticals necessitate a convenient form, such as a powder, which is easy to use and store [4].

This study aimed to determine the optimal conditions for anthocyanin extraction using solvents, followed by an investigation of the effects of spray drying conditions on the production of anthocyanin powder. Additionally, the physicochemical properties of the resulting anthocyanin powder were examined.

2. Materials and Methods

2.1. Materials

Materials: P. frutescens grown under GAP conditions (Phuoc Van town, Can Duoc district, Long An province, Vietnam). After collecting, the fresh leaves were washed to remove the impurities, dried at 60 °C until lower than 10% moisture content, grounded, and sieved through a 0.3 mm sieve. The sample was stored in a PE bag, keeping it protected from light and moisture conditions for all experiments.

Chemicals: Ethanol 99.5% (Merck), chloride acid (36.5%, Merck), potassium chloride (98%, China), sodium acetate trihydrate (99.5%, China), Maltodextrin (MD) 12DE (Sigma-Aldrich). All chemicals and reagents were of analytical grade.

ISSN 2734-9381
https://doi.org/10.51316/jst.178.etsd.2024.34.5.1
Received: Jun 17, 2024; revised: Sep 5, 2024;
accepted: Sep 23, 2024

2.2. Methods

2.2.1. Anthocyanin extraction

1 g sample (according to dry matter) was added to investigate the ratio of ethanol (EtOH), methanol (MeOH), EtOH: HCl: H_2O (EtOH + HCl), MeOH: HCl: H_2O (MeOH + HCl), and H_2O; with solvent concentrations (50%, 60%, 70%, 80%, 90%), adjusted pH of 1 by HCl 1%, and samples and solvent ratios of 1/20(w/v). The extraction was carried out in the laboratory thermostatic water bath 24L (IKA, Germany) at investigated temperatures (40 °C, 50 °C, 60 °C, 70 °C, 80 °C) for investigated intervals of time (30, 60, 90, 120, 150 min) in conditions without light before centrifuging to remove the residue and obtain the supernatant containing anthocyanin. Next, total anthocyanin content (*TAC*) (mg/g) was determined by differential pH method.

2.2.2. Anthocyanin spray-drying

The carrier agent selected for investigation was MD. Lab-scaled spray dryer SD06 Labplant (UK) was utilized for the spray drying process. The appropriate carrier was chosen for further study, with carrier concentration from 15 to 30%, the inlet air temperature ranging from 150 to 180 °C, and the feed flow rate varying from 6 to 9 mL/min, as per the experimental single-factor designs. The resulting anthocyanin powders were then packed in airtight sealed plastic packets and stored in a desiccator for further analysis.

2.2.3. Anthocyanin powder characterization

The Bulk density (*Bd*), Particle density (*Pd*), Tapped density (*Td*), Solubility (*S*), Flowability (*F*), and Porosity (*P*) of the anthocyanin powder were determined according to the description in our previous study [5].

Encapsulation efficiency (EE) was determined via total anthocyanin in total anthocyanin content (*TAC*) and surface anthocyanin content (*SAC*) of the microcapsules [6].

2.2.4. Structural and morphological analysis

Fourier transforms infrared spectroscopy (FT-IR): Analysis was measured via an infrared spectrometer (Tensor 37, Brucker), recording the spectrum between 4000/cm and 450/cm, with a resolution of 1/cm and accumulation of 100 scans (scan rate 0.5/cm/s). Potassium bromide was used in the blank sample.

Scanning electron microscope (SEM): The particle morphology of the obtained anthocyanin powders was analyzed by SEM, JEOL. First, the samples were separately mounted on double adhesive tape stuck on gold aluminum pins. Finally, the individual coated sample was positioned in the SEM machine at an acceleration potential of 2.5 kV to observe the morphology.

X-ray diffraction (XRD): The obtained anthocyanin powders were identified by X-ray diffraction analysis using an X-ray diffractometer (D2 Phaser, Bruker). The crystallinity of anthocyanin spray-drying powder is evaluated by a scanning angle ranging from 30° to 40°. The scanning mode of CuKα radiation nickel filtering with an electrical pressure of 40 kV at a current of 0.8 mA, and a scanning speed of 4° per min.

2.2.5. Anthocyanin content determination

TAC (mg/g) was determined by differential pH method, The anthocyanin samples were measured UV-Vis at 520 nm, and the content was calculated based on mg/g of dry matter following the below equation (1).

$$TAC\ (mg/g) = \frac{A \times D_f \times M_w \times V \times 10^3}{\varepsilon \times L \times m} \qquad (1)$$

with:

A: $(A_{\lambda max} - A_{\lambda 700})_{pH=1} - (A_{\lambda max} - A_{\lambda 700})_{pH=4.5}$;

D_f: Dilution factor; L: Length of cuvette, L = 1 cm;

M_W: Molecular weight of cyanidin 3-glucoside,

M_W = 449.2 g/mol

V: volume of diluted samples (mL); ε: Molar absorptivity ($l.mol^{-1}.cm^{-1}$), ε = 26900 $l.mol^{-1}.cm^{-1}$

m: the weight of the sample (g)

2.2.6. Optimal experimental design

The response surface methodology (RSM) is used to optimize multiple variables simultaneously to achieve the desired response variables. Optimizing the extraction of anthocyanins from *P. frutescens* using Box Behnken Design (BBD) including ethanol concentration (X_1, %), temperature (X_2, °C), and time (X_3, min). A Box-Behnken design (BBD) was used in the optimization of process variables with three factors at three levels with 17 runs, including 5 central points. The following quadratic regression equation (2) is determined by JMP 17.0 software:

$$Y = b_0 + b_1X_1 + b_2X_2 + b_3X_3 + b_{11}X_1^2 + b_{22}X_2^2 + b_{33}X_3^2 + b_{12}(X_1X_2) + b_{13}(X_1X_3) + b_{23}(X_2X_3) \qquad (2)$$

where: $b_0, b_1, b_2, b_3, b_{11}, b_{22}, b_{33}, b_{12}, b_{13}, b_{23}$ are the coefficient of the variable $X_1, X_2, X_3, X_{12}, X_{22}, X_{32}, X_1X_2$, X_1X_3, X_2X_3 correspondingly.

2.2.7. Data analysis

Data were reported as mean ± standard deviation values. The experiments were done in triplicate. The results were analyzed by a one-way analysis of variance (ANOVA) test. Microsoft Excel 2016 and JMP 17.0 Pro software were used for Statistical analysis.

3. Results and Discussion

3.1. Anthocyanin Extraction from P. frutescens

Extraction efficiency depends on the polarity of the solvent and the nature of the material to be captured. Anthocyanins have an aromatic ring, containing -OH, -C=O, or -OCH groups, forming a polar molecule, so they are often extracted with polar organic solvents or mixtures of organic solvents and water. MeOH, EtOH, acetone, and acetonitrile are commonly used organic solvents in extraction processes. These solvents denature membranes and stabilize anthocyanins. In addition, at pH range 1 - 3, anthocyanin color will be more stable, preventing denaturation [7]. Previous studies have shown that acidified alcohol is a suitable solvent for anthocyanin extraction. Therefore, 5 different solvents were chosen in this study including EtOH, MeOH, EtOH + HCl, MeOH + HCl, and H_2O.

Fig. 1A shows that the solvent (EtOH + HCl) outperformed (MeOH + HCl), and resulted in the highest obtained TAC of 1.423 mg/g DM. HCl creates an acidic environment that increases the extraction yield, though strong acids can hydrolyze the glycosidic linkage between anthocyanidin and sugars [8]. However, the use of strong acids can cause hydrolysis of the glycosidic bond, the bond between anthocyanidin, and a sugar moiety, and the presence of strong acids can also cause problems in the further processing of the extracts [9]. These results were in line with findings by Ta Thi To Quyen *et al.* on purple sweet potato anthocyanin extraction using EtOH + HCl [10]. On the other hand, the polarity of the solvent is determined by its dielectric constant and hydrogen bonding values. Water exhibits higher dielectric constant and hydrogen bonding values compared to EtOH. Consequently, mixing EtOH and H_2O results in EtOH-H_2O mixtures with varying degrees of polarity. The anthocyanin content increased from 1.403 mg/g DM (50% EtOH) to 2.221 mg/g DM (70% EtOH). Then, *TAC* declined to 2.042 mg/g DM at 90% EtOH (Fig. 1B). This behavior could be attributed to the presence of hydroxyl groups in anthocyanin molecules, enabling their solubility in H_2O and polar solvents. However, excessively high EtOH concentrations reduce the polarity of the solvent system, consequently diminishing the solubility of extracted anthocyanin. This observation confirmed the influence of solvent polarity on anthocyanin extraction from *P. frutescens* leaves. Furthermore, in (EtOH-H_2O) system, anthocyanin exists in the quinoidal form due to the neutral environment. The presence of sugar moieties attached to the oxygen atom at C3 and C5 in anthocyanin molecules enhances their solubility in water. This explains why decreasing the concentration ratio leads to a corresponding increase in the color absorption of the extract, reaching a maximum of 70% EtOH. In contrast, when in the quinoidal form, enol-ketone resonance can occur at the OH groups on carbon C7 of ring A and carbon C4 of ring B [11]. This reduces the water solubility of the anthocyanin molecule. In this case, the aglycone portion of the anthocyanin molecule exhibits better solubility in EtOH.

As temperature increases, solvent viscosity decreases, improving solvent penetration through the material, expanding the contact area, and enhancing extraction [7]. Fig. 1C shows that *TAC* increased from 1.669 mg/g DM (40 ℃) to 2.876 mg/g DM (60 ℃). However, it decreased at higher temperatures, reaching 2.718 mg/g DM (70 ℃) and 2.566 mg/g DM (80 ℃), However, when the temperature is increased to too high a level, it will cause a loss of *TAC* because of the oxidation of anthocyanin. Thus, 60 ℃ is the suitable temperature for anthocyanin extraction. Additionally, extraction time influences anthocyanin yield. If time is too short, the solvent may not fully dissolve the anthocyanins; if time is too long, it can lower product quality by dissolving other substances and causing anthocyanin degradation due to prolonged high temperatures.

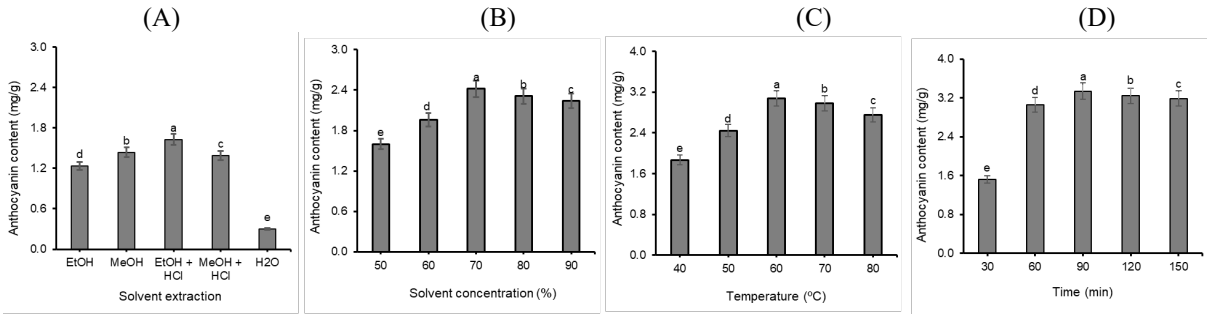

Fig. 1. Effects of solvent extraction (A), solvent concentration (B), temperature (C), and time (D) on anthocyanin extraction

Note: Within the same graph, different letters on columns represent statistically significant differences ($p < 0.05$)

The obtained *TAC* increased, peaking at 3.145 mg/g DM at 90 min, then slightly declined to 2.986 mg/g DM (Fig. 1D). Insufficient time hinders solvent dissolution, while prolonged extraction causes thermal instability and degradation, which can lower the solution purity [7]. In short, in this study, the system of (EtOH + HCl) with 70% EtOH was chosen for anthocyanin extraction from *P. frutescens* leaves. The extraction was done at 80 ℃ for 90 min.

Through the factors obtained from the above survey experiments, the experimental domain of 3 optimal parameters including X_1-Ethanol concentration: 60÷70%, X_2 - Temperature: 50÷70 ℃, X_3 - Time: 60÷120 min.

3.2. Optimizing Anthocyanin Extraction Conditions

The anthocyanin extraction from *P. frutescens* was further optimized through RMS. X_1, X_2, and X_3 were independent variables, namely, ethanol concentration, temperature, and time, respectively. The responses function (Y: *TAC*) was partitioned into linear, quadratic, and interactive components. Experimental data were fitted to the second-order regression in (2). The different combinations of the three factors (ethanol concentration, extraction temperature, and extraction time) and experimental and predicted values of *TAC* are given in Table 1. Indeed, the coefficient of determination was very high (max $R^2 = 0.98$) denoting that *TAC* models have a high level of explanation (Table 2).

Table 1. Experimental design and results

No.	Coded			Actual			Y
	X_1	X_2	X_3	Ethanol concentration (%)	Temperature (℃)	Time (min)	TAC (mg/g DM)
1	-1	-1	0	60	50	90	2.951
2	-1	1	0	60	70	90	3.122
3	1	-1	0	80	50	90	3.118
4	1	1	0	80	70	90	3.213
5	0	-1	-1	70	50	60	3.184
6	0	-1	1	70	50	120	3.012
7	0	1	-1	70	70	60	3.095
8	0	1	1	70	70	120	3.281
9	-1	0	-1	60	60	60	3.113
10	1	0	-1	80	60	60	3.192
11	-1	0	1	60	60	120	2.936
12	1	0	1	80	60	120	3.158
13	0	0	0	70	60	90	3.367
14	0	0	0	70	60	90	3.314
15	0	0	0	70	60	90	3.345
16	0	0	0	70	60	90	3.366
17	0	0	0	70	60	90	3.401

Table 2. Regression coefficients for total anthocyanin content of *P. frutescens* extract

Term	Coefficient	The standard error for the coefficient	t ratio	*P* value
Intercept	3.36	0.02	184.64	<.0001*
X1	0.07	0.01	4.86	0.0018*
X2	0.05	0.01	3.88	0.0061*
X3	-0.02	0.01	-1.71	0.1306
X1*X2	-0.02	0.02	-0.93	0.3813
X1*X3	0.04	0.02	1.76	0.1222
X2*X3	0.08	0.02	4.40	0.0032*
X1* X1	-0.15	0.01	-7.59	0.0001*
X2*X2	-0.11	0.01	-5.41	0.0010*
X3*X3	-0.11	0.01	-5.47	0.0009*
*Variables with P value ≤ 0.05 (marked with *) are variables that affect the objective function Y of the equation.*				

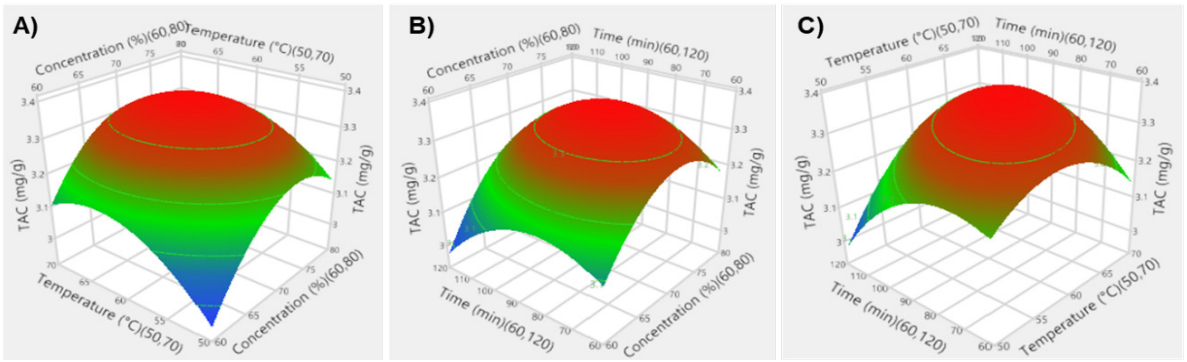

Fig. 2. Effects on anthocyanin content of the interaction between concentration - temperature (A), time - concentration (B), time - temperature (C)

Table 3. Adjustment analysis of the models

Source	*DF*	*SS*	*MS*	*F* Ratio
Model	6	0.31	0.05	22.54
Error	10	0.02	0.002	*P value* > *F*
C. Total	16	0.33		<0.0001*
Lack Of Fit	6	0.01	0.003	3.07
Pure Error	4	0.004	0.001	*P value* > *F*
Total Error	10	0.02		0.1483
			Max *RSq*	0.98
DF: degree of freedom; SS: sum of squares; MS: mean square				

The suitable model is the quadratic model, and the regression equation has the following form using coded variables:

$$Y = 3.36 + 0.07X_1 + 0.05X_2 + 0.08X_2X_3 - 0.15X_1^2 - 0.11X_2^2 - 0.11X_3^2 \quad (3)$$

After analysis of variance and based on *F* and *P* values, a second-order polynomial response surface model (3) and Table 3 were fitted to the response variable (*Y*). The equation (3) indicated that ethanol concentration (X_1) and extraction temperature (X_2), positively affects *TAC*. At the same time, the negative impact was recorded with concentration (X_1), temperature (X_2), and the quadratic time (X_3). The non-significant value of lack of fit ($F = 3.07$) showed the model is fitted with a good prediction (the values of max $R^2 = 0.98 > 0.8$) (Table 3) at level 0.05. In addition, the counterplots of response surfaces for extraction are presented in Fig. 2.

Based on the above results, the quadratic models were appropriate for estimating anthocyanin content in this experimental condition. The maximal anthocyanin content predicted by the models and the optimal conditions are presented in Table 4.

The results showed no significant difference between predicted and experimental anthocyanin. This indicated that the experimental model was suitable for practical experiments.

Table 4. Maximum values of anthocyanin content from a prediction by model and experiment at optimal extracting conditions.

Optimal extraction conditions			Predicted contents (mg/g DM)	Experimental contents (mg/g DM)
Ethanol (%)	Temperity (℃)	Time (mins)		
72	63	90	3.373	3.306

3.3. Spray Drying for Obtaining Anthocyanin Powder

Spray drying aimed to enhance the stability of anthocyanin powder. The effects of carrier concentration, inlet feed flow rate, and temperature were shown in Fig. 3.

Fig. 3A reveals that the encapsulation efficiency increased to 63.2% at 25% carrier agent and decreased to 61.55% at 30%. In fact, MD acts as a bulking agent in the spray drying process, enhancing the recovery efficiency of the dried powder. However, excessively high solids concentration, which increased the viscosity of the solution, hindered the drying process and affected product quality and recovery efficiency. At lower MD supplementation levels, the product adheres excessively to equipment walls, leading to low product recovery efficiency while higher maltodextrin concentration resulted in higher moisture content in the anthocyanin powder and lower recovery efficiency [12]. Besides, the encapsulation efficiency increased from 42.93% to 56.48% as spray drying temperature rose from 150 ℃ to 160 ℃. However, a higher drying temperature of 180 ℃ resulted in a decline in recovery efficiency to 49.59% (Fig. 3B). This suggests that excessively low or high drying air temperatures adversely affect obtained anthocyanin powder efficiency. At low drying temperatures, the drying time for feed particles extends until they become light enough to be collected by the cyclone. Consequently, the residence time of feed particles in the drying chamber increases. Moreover, the high moisture content of the feed causes high product stickiness, increasing the risk of nozzle clogging and powder adhesion to equipment walls, thereby reducing product recovery efficiency. However, excessively high temperatures cause excessive evaporation of moisture from the feed, leaving only a small amount of moisture in the form of strong bonds, making it difficult for moisture to escape. Therefore, the moisture content reduction is negligible. Additionally, high temperatures impact heat-sensitive anthocyanins, which may partially burn and adhere to equipment walls, reducing product recovery efficiency. This finding aligns with a report of S. Santhalakshmy that drying temperatures around 160-190 ℃ produced products with satisfactory color and quality [13].

Fig. 3C reveals that increasing the inlet feed flow rate reduces the residence time of the drying material in the drying chamber, accordingly, leading to lower drying efficiency and anthocyanin degradation. Moreover, it resulted in higher moisture content and an increase in the amount of moist particles adhering to the drying chamber walls, further decreasing product recovery efficiency after spray drying. While a slightly lower moisture content was obtained at an inlet feed flow rate of 6 mL/min, the equipment's unstable operation and extended drying time under this condition prompted us to select an inlet feed flow rate of 7 mL/min for subsequent experiments. Under this condition, the spray drying product recovery efficiency reached 57.41%, and the product moisture content was 4.37%. The findings were in agreement with the study of Jafari *et al*., pomegranate juice powders produced at 25% MD level and 124 ℃, with a high water solubility index of 95%, high density of 0.889 g/cm^3, and *TAC* of 8 mg/L [14].

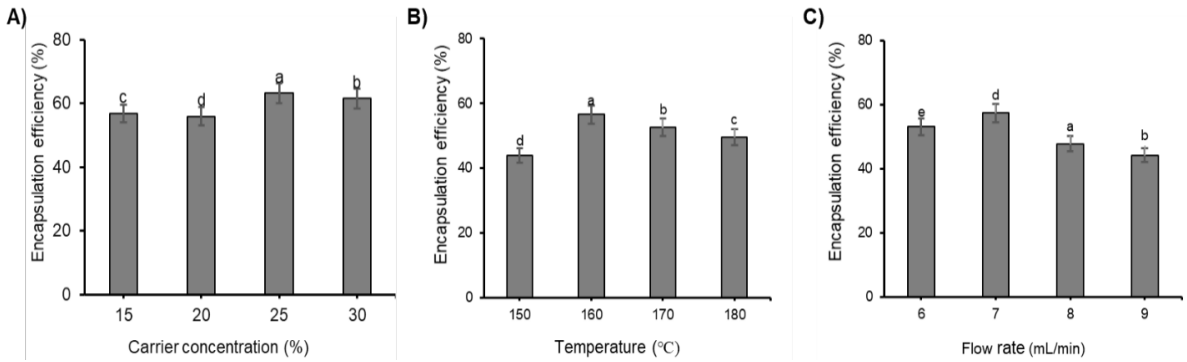

Fig. 3. Effects of carrier agent concentration (A), temperature (B) and flow rate (C) on encapsulation efficiency

In summary, the spray drying conditions for obtaining anthocyanin powder were 160 ℃ and an inlet feed flow rate of 7 mL/min while using carrier agent concentration was 25%.

3.4. Characterization of Anthocyanin Powder

3.4.1. Physicochemical properties of spray-dried anthocyanin powder

The physicochemical properties of the obtained anthocyanin powder, including moisture content, bulk density, particle density, porosity, flowability, solubility, and encapsulation efficiency, were determined. The results are presented in Table 5.

Table 5. Physicochemical properties of spray-dried anthocyanin powder from *P. frutescens*

No.	Criteria	Unit	Results
1	Moisture	%	7.24 ± 0.18
2	Bulk density	g/cm^3	0.23 ± 0.04
3	Particle density	g/cm^3	0.84 ± 0.23
4	Tapped density	g/cm^3	0.26 ± 0.37
5	Flowability	CI (%)	11.54 ± 0.98
		HR	1.08 ± 0.42
6	Porosity	%	69.05 ± 0.86

3.4.2. Scanning electron microscopy

SEM analysis of anthocyanin-enriched dried powder from processed perilla leaves is presented in Fig. 4. The presence of predominant spherical particles with rough or pitted surfaces. The formation of these surface indentations on spray-dried particles is generally attributed to particle shrinkage resulting from severe moisture loss during the cooling process. The particles with smooth spheres were similar to that of polyphenol microcapsules extracted from *Orthosiphon stamineus* leaves [15]. According to Ferrari *et al*. (2012), particles with rough surfaces can contribute to increased moisture content and reduced pigment retention capacity [16]. Additionally, Silva *et al.* (2013) suggested that particles with rough surfaces have a larger surface area compared to smooth particles, potentially making them more susceptible to degradation reactions such as oxidation [17]. Fig. 4. SEM micrographs of the anthocyanin-enriched dried powder from perilla leaves at different magnifications: (A) 2,000x, (B) 5,000x, (C) 10,000x.

3.4.3. X-ray diffraction analysis

XRD was used to determine the nature of samples, whether they were crystalline or amorphous in nature. The XRD pattern of spray-dried Anthocyanin from *P. frutescens* leaves is presented in Fig. 5.

The presence of high-intensity peaks at 2θ angles of 20° and 32° indicates the amorphous nature of the powder. Upon further observation, the absence of any sharp peaks confirms the absence of any ordered crystalline structures in the XRD pattern (Fig. 5). In the amorphous state, molecules are arranged in a disordered manner, resulting in dispersed bands. In contrast, crystalline materials exhibit sharp and defined peaks due to their highly ordered structure where the XRD patterns of the powder samples showed a broad peak, the intensity gradually diminishes with no subsequent sharp peaks, consistent with the low-intensity scattering properties of amorphous compounds. The observed amorphous nature of the powder is attributed to the fact that carrier materials (MD) used possess amorphous characteristics [18]. Thus, the XRD data for this anthocyanin powder indicates that the compounds exist in an amorphous state. This implies that anthocyanin molecules do not arrange in a repetitive order but are randomly distributed, resulting in a non-crystalline structure. XRD spectral analysis of anthocyanin perilla leaf powder serves as a measure of sample purity and helps in identifying the characteristics of the crystalline material.

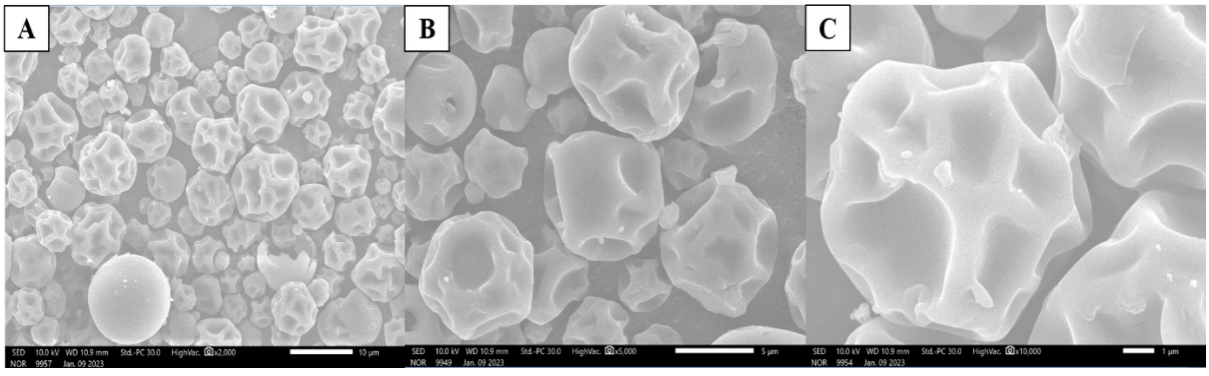

Fig. 4. SEM micrographs of the anthocyanin-enriched dried powder from perilla leaves at different magnifications: (A) 2,000x, (B) 5,000x, (C) 10,000x.

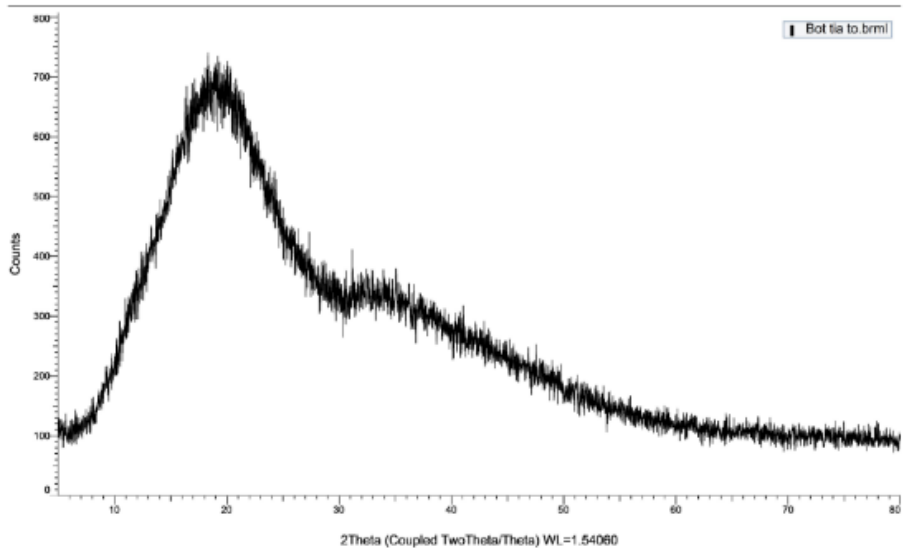

Fig. 5. XRD pattern of spray-dried anthocyanin powder

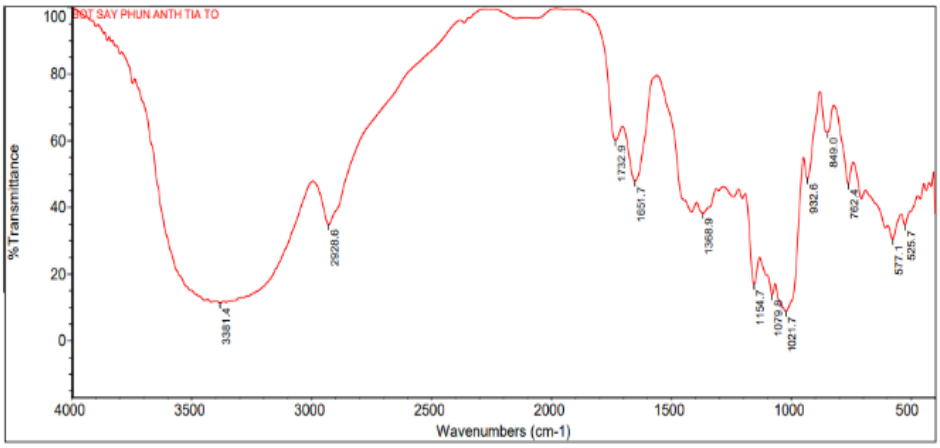

Fig. 6. FT-IR Spectrum of anthocyanin powder

3.4.4. FT-IR analysis

To gain insights into the potential intermolecular interactions between the carrier material and the spray-dried powder, FT-IR spectroscopy was employed. The FT-IR spectrum of the spray-dried powder revealed the presence of characteristic absorption bands at 3381.4, 2928.6, 1732.9, 1651.7, 1368.9, 1154.7, 1079.8, 1021.7, 932.6, 849, and 762.4 cm^{-1}. These bands provide valuable information about the functional groups and molecular interactions present within the powder.

Fig. 6 shows that the broad bands in the spectral region 3500-3000 cm^{-1} corresponded to -OH groups, while the bands at 2928.6 cm^{-1} were the result of vibrations elongation dynamics of the C-H bond. A band at 1732.9 cm^{-1} was assigned to the stretching vibrations of the aromatic ring, which is characteristic of anthocyanins [18]. The peak of 1651.7 cm^{-1} (COO- characteristic carboxyl groups in the anthocyanin structure. The frequency band at 1368.9 cm^{-1} corresponded to the C-O deformation of phenol. At 1154.7 and 1079.8 cm^{-1} were assigned to the stretching of the C-O-C bond. Another band at 1021.7 cm^{-1} corresponds to the stretching of the C-O bonds of phenol. The dried powder sample contained maltodextrin and had a frequency band at 932.6 cm^{-1} that was attributed to the C-O stretching of C-O-C groups in the anhydroglucose ring, and at 849 and 762.4 cm^{-1} due to C-H bend and ring wrinkle [19, 20]. FT-IR analyses showed that the obtained microparticles were chemically and thermally stable systems for encapsulating perilla anthocyanins. Strong interactions between the carrier and sample that could reduce the encapsulation efficiency and stability of anthocyanins were not observed during spray drying. Furthermore, the functional and technological properties of the microparticles were improved.

4. Conclusion

In this study, the method of extracting anthocyanin found the optimal implementation of the three selected factors using the Box Behnken model and JMP 17 Pro software to plan experiments, analyze,

and process data. The results showed that when extracted with 72% ethanol at 63 ℃ in 90 min, the optimal anthocyanin content was 3.373 mg/g DM. The predicted contents align well with a first-order model (max R^2 = 0.98) and are equivalent to experiment values (3.306 mg/g DM). Spray-drying conditions to obtain the anthocyanin powder from *Perilla. frutescens* extract with 25% maltodextrin concentration, at 160 ℃ and 7 mL/min of inlet feed flow rate. The characteristics of the obtained anthocyanin powder were evaluated under a SEM, XRD, and FT-IR, showing that the microencapsulation process was carried out effectively. This finding offers a platform for further studies and applications of anthocyanin powder from this material.

References

[1] H. M. Ahmed, Ethnomedicinal, Phytochemical and pharmacological investigations of perilla frutescens (L.) britt, Molecules, vol. 24, no. 1, Dec. 2018. https://doi.org/10.3390/molecules24010102

[2] G. K. Oguis, E. K. Gilding, M. A. Jackson, and D. J. Craik, Butterfly pea (clitoria ternatea), a cyclotide-bearing plant with applications in agriculture and medicine, Front Plant Sci, vol. 10, May. 2019. https://doi.org/10.3389/fpls.2019.00645

[3] A.C. Goncalves, A.R. Nunes, A. Falcao, G. Alves, and L.R. Silva, Dietary effects of anthocyanins in human health: a comprehensive review, Pharmaceuticals (Basel), vol. 14, iss. 7, Jul. 2021. https://doi.org/10.3390/ph14070690

[4] T. Coultate and R.S. Blackburn, Food colorants: their past, present and future, Coloration Technology, vol. 134, iss. 3, Mar. 2018, pp. 165-186. https://doi.org/10.1111/cote.12334

[5] N. T. N. Hoang, N. N. K. Nguyen, L. T. K. Nguyen, A. T. H. Le, and D. T. A. Dong, Research on optimization of spray drying conditions, characteristics of anthocyanins extracted from *Hibiscus sabdariffa* L. flower and application to marshmallows, Food Science & Nutrition, vol. 12, iss. 3, Jan. 2024, pp. 2003-2015. https://doi.org/10.1002/fsn3.3898

[6] S. Akhavan Mahdavi, S. M. Jafari, E. Assadpoor, and D. Dehnad, Microencapsulation optimization of natural anthocyanins with maltodextrin, gum Arabic and gelatin, International Journal of Biological Macromolecules, vol. 85, Apr. 2016, pp. 379-385. https://doi.org/10.1016/j.ijbiomac.2016.01.011

[7] Z. Zhu *et al*., Green ultrasound-assisted extraction of anthocyanin and phenolic compounds from purple sweet potato using response surface methodology, Int Agrophysics, vol. 30, no. 1, 2016. https://doi.org/10.1515/intag-2015-0066

[8] S. Oancea, M. Stoia, and D. Coman, Effects of extraction conditions on bioactive anthocyanin content of *Vaccinium Corymbosum* in the perspective of food applications, Procedia Engineering, vol. 42, 2012, pp. 489-495. https://doi.org/10.1016/j.proeng.2012.07.440

[9] S. Silva, E. M. Costa, C. Calhau, R. M. Morais, and M.E. Pintado, Anthocyanin extraction from plant tissues: a review, Critical Reviews Food Science Nutrition, vol. 57, iss. 14, May. 2017, pp. 3072-3083. https://doi.org/10.1080/10408398.2015.1087963

[10] T. T. T. Quyen, H. T. K. Cuc, C. T. N. Thuy, and D. H. Cuong, Extraction of Anthocyanins Pigment From Purple Sweet Potatoes, J Sci and Technol DaNang, vol. 11, 2014.

[11] J. S. Boeing, E. O. Barizao, P. F. Montanher, V. de Cinque Almeida, and J. V. Visentainer, Evaluation of solvent effect on the extraction of phenolic compounds and antioxidant capacities from the berries: application of principal component analysis, Chem Central Journal, vol. 8, Aug. 2014. https://doi.org/10.1186/s13065-014-0048-1

[12] T. Huynh, C. Kha, V. Nguyen, T. Nguyen, T. Ha, and H. Ngo, Spray drying conditions of lime juice prepared by freeze-concentration, IOP Conference Series: Earth and Enviromental Science, IOP Publishing, 2023, vol. 1155, no. 1, pp. 012017. https://doi.org/10.1088/1755-1315/1155/1/012017

[13] S. Santhalakshmy, S. J. Don Bosco, S. Francis, and M. Sabeena, Effect of inlet temperature on physicochemical properties of spray-dried jamun fruit juice powder, Powder Technology, vol. 274, Apr. 2015, pp. 37-43. https://doi.org/10.1016/j.powtec.2015.01.016

[14] S. M. Jafari, M. Ghalegi Ghalenoei, and D. Dehnad, Influence of spray drying on water solubility index, apparent density, and anthocyanin content of pomegranate juice powder, Powder Technology, vol. 311, Apr. 2017, pp. 59-65. https://doi.org/10.1016/j.powtec.2017.01.070

[15] S. F. Pang, M. M. Yusoff, and J. Gimbun, Extraction and microencapsulation of polyphenols from orthosiphon stamineus leaves, Journal of Mechanical Engineering and Science (JMES), vol. 7, Dec. 2014, pp. 1033-1041. https://doi.org/10.15282/jmes.7.2014.2.0100

[16] C. C. Ferrari, S. P. M. Germer, and J. M. de Aguirre, Effects of spray-drying conditions on the physicochemical properties of blackberry powder, Drying Technolpgy, vol. 30, iss. 2, Nov. 2011, pp. 154-163. https://doi.org/10.1080/07373937.2011.628429

[17] C. I. Piñón-Balderrama, C. Leyva-Porras, Y. Terán-Figueroa, V. Espinosa-Solís, C. Álvarez-Salas, and M.Z. Saavedra-Leos, Encapsulation of active ingredients in food industry by spray-drying and nano spray-drying tech, Processes, vol. 8, iss. 8, 2020. https://doi.org/10.3390/pr8080889

[18] A. S. Asnawi, M. H. Hamsan, M. F. Kadir, S. B. Aziz, and Y. M. Yusof, Investigation on electrochemical characteristics of maltodextrin - methyl cellulose electrolytes, Molecular Crystals and Liquid Crystals, vol. 708, iss. 1, Jan. 2021, pp. 63-91. https://doi.org/10.1080/15421406.2020.1810954

[19] M. Mehran, S. Masoum, and M. Memarzadeh, Improvement of thermal stability and antioxidant

activity of anthocyanins of Echium amoenum petal using maltodextrin/modified starch combination as wall material, International Journal of Biological Macromolecules, vol. 148, Apr. 2020, pp. 768-776. https://doi.org/10.1016/j.ijbiomac.2020.01.197

[20] S.E.M. Kalajahi and S. Ghandiha, Optimization of spray drying parameters for encapsulation of Nettle (*Urtica dioica* L.) extract, LWT, vol. 158, Mar. 2022. https://doi.org/10.1016/j.lwt.2022.113149